ELSEVIER

Chemical Geology 187 (2002) 267–277

CHEMICAL GEOLOGY
INCLUDING
ISOTOPE GEOSCIENCE

www.elsevier.com/locate/chemgeo

The Zedong terrane: a Late Jurassic intra-oceanic magmatic arc within the Yarlung–Tsangpo suture zone, southeastern Tibet

Isabella R.C. McDermid[a,*], Jonathan C. Aitchison[a], Aileen M. Davis[a], T. Mark Harrison[b], M. Grove[b]

[a]*Tibet Research Group, Department of Earth Sciences James Lee Science Bldg., University of Hong Kong, Pokfulam Road, Hong Kong, SAR, China*
[b]*Department of Earth and Space Sciences and IGPP, University of California, Los Angeles, CA 90095, USA*

Received 1 October 2001; accepted 21 March 2002

Abstract

An overturned sequence of igneous and volcaniclastic rocks crops out along the Yarlung–Tsangpo suture zone (YTSZ), in southeastern Tibet. These rocks are remnants of an intra-oceanic island arc, the Zedong terrane, that once lay between India and Asia. $^{40}Ar/^{39}Ar$ dating and U–Pb ion microprobe analyses reported here reveal that this arc was active during the Jurassic. U–Pb dating of zircon from a dacite breccia from the middle portion of the Zedong terrane, yields an age of 161 ± 2.3 Ma (1σ). $^{40}Ar/^{39}Ar$ dating of hornblende from a cross-cutting andesite dyke yields the youngest age of 152.2 ± 3.3 Ma (1σ). $^{40}Ar/^{39}Ar$ results from hornblende from andesite dykes and an andesite breccia from the upper portion yield a mean age of 156 ± 0.3 Ma (1σ). Additional U–Pb and $^{40}Ar/^{39}Ar$ dating of zircon and hornblende from quartz diorite yields a mean age of 156.8 ± 0.8 Ma (1σ). Geochronological data reported here and other published work indicate that the intra-oceanic subduction system to which the Zedong terrane belonged was active from at least Late Jurassic to Early to mid Cretaceous.

Keywords: Tethys; Yarlung–Tsangpo suture zone; Island arc; Zedong terrane; Jurassic; Geochronology

1. Introduction

The Yarlung–Tsangpo suture zone (YTSZ), of southeastern Tibet, is the youngest and southernmost suture that formed during the Indo-Asian collision and it contains remnants of material that once lay between India and Asia prior to continental collision (Fig. 1). The three terranes that have been recognized within the YTSZ appear to comprise remnants of a Tethyan intra-oceanic convergent margin (Aitchison et al., 2000). These entities, the Zedong, Dazhuqu and Bainang terranes, are respectively interpreted to represent the magmatic arc, fore-arc ophiolite and subduction complex that developed above a northward subducting slab. Arc volcanic rocks exposed near Zedong are believed to be remnants of the magmatic arc (Fig. 2). As rocks within the YTSZ have been mapped in detail only between Lhaze and Luobusa (Fig. 1), it is not known if additional Zedong terrane

* Corresponding author. Tel.: +852-28578558; fax: +852-25176912.
E-mail address: Isabellm@hkusua.hku.hk (I.R.C. McDermid).

0009-2541/02/$ - see front matter © 2002 Published by Elsevier Science B.V.
PII: S0009-2541(02)00040-2

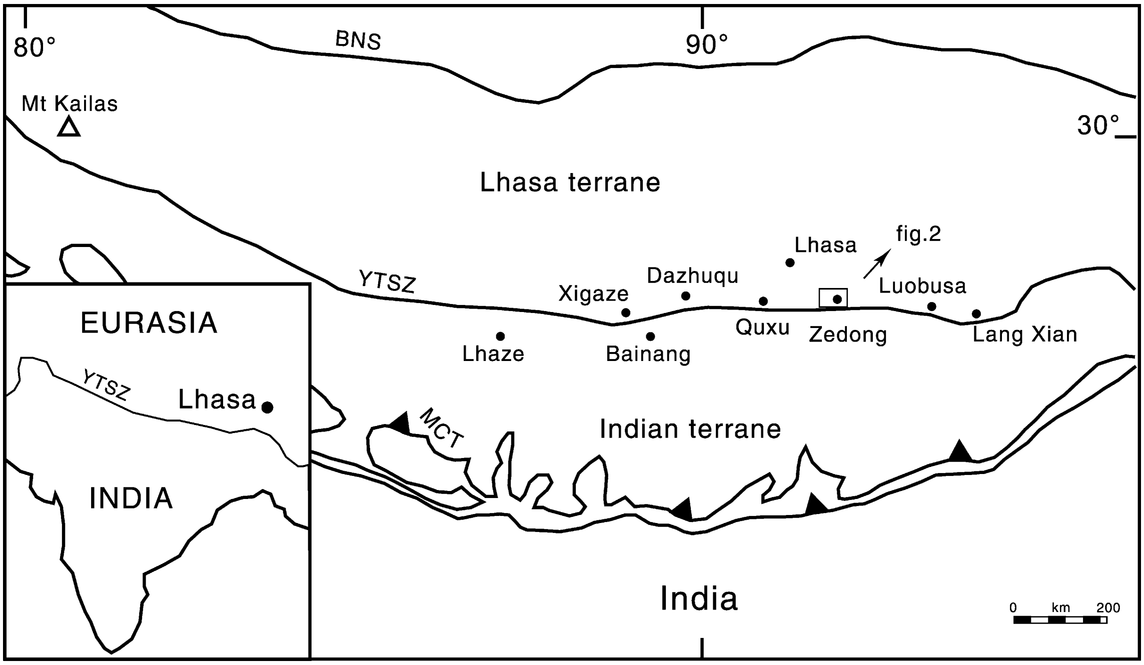

Fig. 1. Simplified map of southern Tibet showing the position of the Yarlung–Tsangpo suture zone (YTSZ), the Bangong-Nujiang suture zone (BNS) and key localities within the suture. The YTSZ is the southern most suture separating the Indian and Asian microcontinental fragments.

rocks occur elsewhere along the suture. Other rocks of island arc affinity have been identified further west along the Indus suture zone, in Kohistan (Dras and Chalt groups) and in Ladakh (Spong arc). The oldest arc volcanics from the Kohistan island arc and Spong arc are Cretaceous (Searle et al., 1999; Corfield et al., 2001; Pedersen et al., 2001) and considerably younger than those reported herein.

Previous studies of the intra-oceanic subduction system associated with the Zedong terrane indicated that this system was active in the Early to mid Cretaceous (Aitchison et al., 2000 and references therein). Geochronologic evidence presented in this paper from igneous rocks of the Zedong terrane extends the known duration of intra-oceanic magmatic arc activity back to the Late Jurassic. Our new geochronological data combined with previous palaeontological data suggest that the associated subduction system was longer-lived than previously thought and is in accord with the interpretation of tomographic imaging beneath the area, which indicates the presence of a considerable length of subducted oceanic lithosphere (Van der Voo et al., 1999).

2. Geological setting

Intra-oceanic island arc rocks of the Zedong terrane are exposed south of the Yarlung Tsangpo in a discontinuous pattern that extends eastward from the Sam Ye ferry crossing past the Zedong township (Fig. 2). Lithologies typical of the Bainang and Dazhuqu terranes are also exposed in this area. Similar rocks correlative to those of the Zedong terrane are also exposed further to the east around Luobusa (Zhou et al., 1996).

Suture zone rocks are exposed south of the Lhasa terrane and north of a series of overlying thrust sheets, which developed during the India–Asia collision and elsewhere obscure Tethyan remnants (Badengzhu, 1979). These thrusts are associated with the Great counter thrust system (Heim and Gansser, 1939; Gansser, 1964), which marks the southern boundary of the YZSZ in southeastern Tibet and separates Tethyan rocks from those representing the distal northern continental margin of India (Fig. 1). This fault system is locally referred to as the Renbu–Zedong thrust system (RZTS) (Yin et al., 1994,

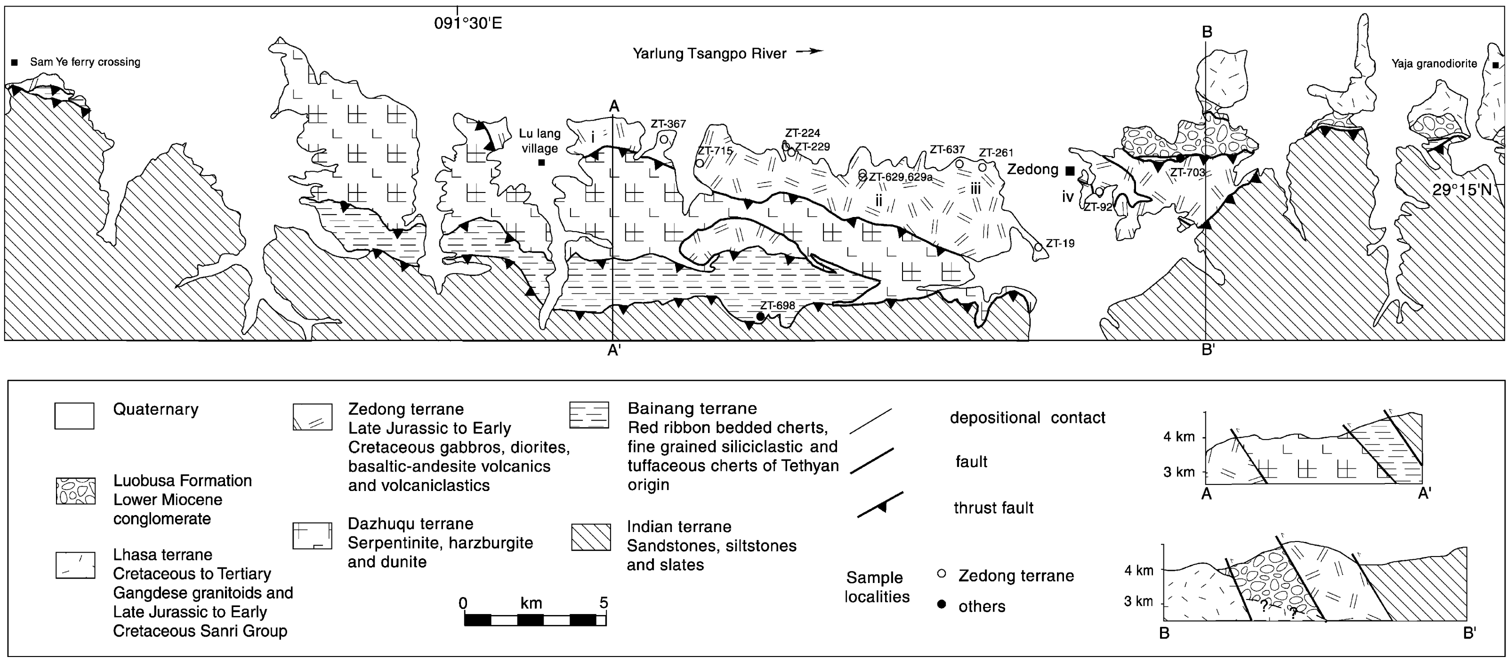

Fig. 2. Simplified geological map of the Zedong area showing the distribution of terranes and sample localities (drafted from Tibet Ministry of Geology 1:50,000 base maps and own field observations (Badengzhu, 1979; Aitchison et al., 2000). All contacts between terranes are faults and where known the sense of displacement is shown. Cross sections A–A′ and B–B′ show the geometry of the Zedong, Dazhuqu and Bainang terranes relative to the Lhasa (Asian) and Indian terranes. i–iv refer to the locations of schematic stratigraphic sections in Fig. 3.

1999). At Zedong it consists of a series of south-dipping thrusts that place Upper Triassic sandstones and phyllites of Indian affinity over fragments of the intra-Tethyan subduction system and syn-India–Asia collision-related sediments (Badengzhu, 1979; Yin et al., 1994, 1999). The Zedong area has been interpreted as a structural window framed, to the north, by the Gangdese thrust (GT) and to the south by the Renbu–Zedong thrust system (RZTS) (Harrison et al., 2000; Quidelleur et al., 1997; Yin et al., 1994, 1999).

Detailed geochronological studies around Zedong constrain the timing of displacement on the RZTS and uplift of Gangdese granitoids (Harrison et al., 2000; Quidelleur et al., 1997; Yin et al., 1994, 1999). $^{40}Ar/^{39}Ar$ thermochronology and U–Pb geochronology along the RZT near Lang Xian (Fig. 2), east of Zedong, indicate that the RZT was active between 19 and 11 Ma (Quidelleur et al., 1997). Harrison et al. (2000) systematically sampled granitoids from east of the Zedong township where U–Pb dating of zircon from the Yaja granodiorite, overlain by conglomerates of the Luobusa Formation, yielded a crystallization age of 30.4 ± 0.4 Ma.

Rocks exposed between those of Asian affinity (Lhasa terrane) and those of Indian affinity have previously been mapped as undifferentiated chert-dominated mélange (Yin et al., 1999). They describe the mélange as consisting of chert, shale, marble, andesite, diorite, serpentinite, gabbro, limestone, phyllite and volcanic breccia. However, detailed mapping by the Xizang Geological Survey (Badengzhu, 1979) and as part of this investigation reveals that, although zones of both serpentinite-matrix and mud-matrix mélange exist locally, many suture zone rocks within the Zedong area are generally stratigraphically coherent. Specifically, three intra-oceanic terranes (the Zedong, Dazhuqu, and Bainang terrane) and a post-collision sedimentary unit (the upper Oligocene–lower Miocene Luobusa Formation) can be recognized within the YTSZ at Zedong. All are juxtaposed against one another along south-dipping thrusts associated with the RZTS. Locally, Miocene conglomerates of the Luobusa Formation unconformably overlie the Lhasa terrane and suture zone rocks. Elsewhere it has been thrust northward over suture zone rocks along the RZTS (Aitchison et al., in press).

3. Intra-Tethyan convergent plate boundary

The Dazhuqu, Bainang and Zedong terranes represent an ophiolite, a subduction complex and a magmatic arc of a formerly active, south-facing, intra-oceanic arc subduction system that formed within Tethys. Vestigial remnants of this plate boundary have been identified at Zedong and elsewhere along the Yarlung–Tsangpo suture in southern Tibet.

3.1. Dazhuqu terrane—ophiolite

Ophiolitic rocks that occur along the YTSZ in southern Tibet are assigned to the Dazhuqu terrane (Aitchison et al., 2000). Almost complete ophiolitic sequences occur in the vicinity of Zedong, Luobusa and Xigase (Fig. 1) (Aitchison et al., 2000; Hérbert et al., 2000; Zhou et al., 1996). Serpentinised harzburgite, gabbro, dunite and rare pillow lavas crop out in the Zedong area. Petrographic and geochemical data suggesting that these rocks once comprised a supra-subduction assemblage basement formed during intra-oceanic subduction are in agreement with studies of similar rocks at Luobusa and Xigase (Girardeau et al., 1985; Pearce and Deng, 1988; Hérbert et al., 2000; Zhou et al., 1996). Radiolarian biostratigraphy indicates late Barremian–early Aptian deposition of supra-ophiolite sediments at several localities in the vicinity of Xigase (Zyabrev et al., 1999). Paleomagnetic studies of the Cretaceous supra-ophiolite deposits at Dazhuqu (Fig. 1) indicate the Dazhuqu terrane formed at a subequatorial location (Abrajevitch et al., 2001).

3.2. Bainang terrane—subduction complex

The Bainang terrane is an imbricate thrust stack containing numerous tectonic slices of red ribbon-bedded cherts, fine-grained siliciclastics and tuffaceous cherts of Tethyan origin. The terrane is well exposed in the Donghla, Xialu, Bainang and Zedong districts. At Zedong and elsewhere, it is always positioned to the south of the Dazhuqu terrane, and is in fault contact with both the Dazhuqu terrane and rocks of Indian affinity. Unlike exposures of the Bainang terrane studied elsewhere (Ziabrev et al., 2001), a clastic-dominated succession is also present at Zedong.

Radiolarian and conodont biostratigraphy (Ziabrev et al., 2001; Bally et al., 1980; Wu, 1993) have revealed that most of the red ribbon-bedded cherts are Triassic to Jurassic and even Lower Cretaceous. Fine-grained clastic sediments overlying the cherts at Bainang are typically mid Cretaceous (mid Aptian) (Zyabrev et al., 2000). The structural style of the Bainang terrane is similar to that of a subduction complex associated with a south-facing convergent margin (Aitchison et al., 2000).

3.3. Zedong terrane—magmatic arc

The Zedong terrane, first described by Aitchison et al. (2000), is a fault-bounded unit that incorporates igneous and volcaniclastic rocks including basaltic–andesitic pillow lavas, breccias, tuffs, flows, cherty tuffs, dacites, rhyolites, gabbros, diorites and quartz diorites. Rare crystalline limestone blocks also occur within highly deformed andesitic tuffs. Most rocks have experienced sub-greenschist grade metamorphism. Autoclastic and epiclastic andesitic breccias are the dominant rock type within the Zedong terrane. These breccias are locally intruded by numerous basaltic–andesite, and dacite dykes. Basaltic andesites are hornblende-phyric and are unlike the plagioclase-phyric andesites typical of the Lhasa terrane exposed on the north side of the Yarlung Tsangpo. Preliminary geochemistry indicates that volcanic rocks formed in an intra-oceanic island arc setting (McDermid et al., 2001; 2002, in preparation).

Two representative stratigraphic sections within the Zedong terrane reveal characteristics of formation in an oceanic setting. At Lu Lang (~ 15 km west of

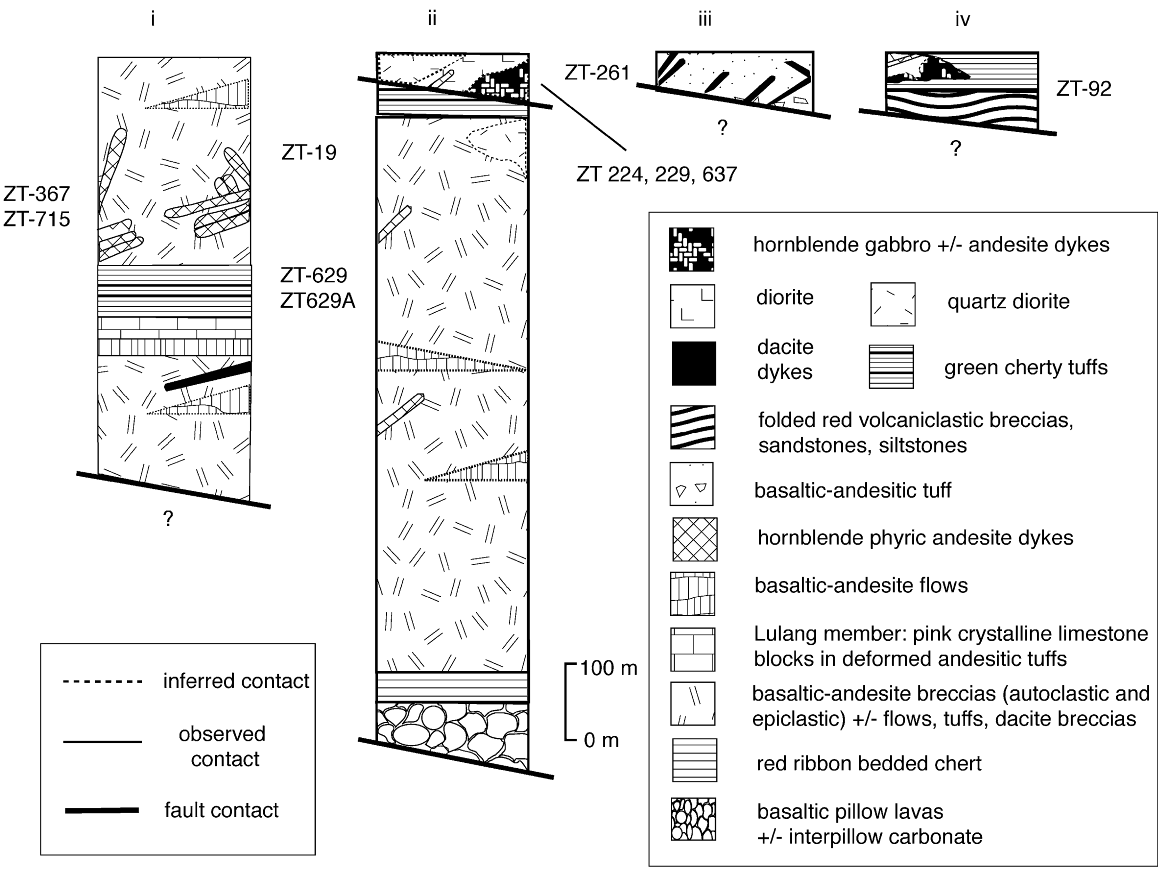

Fig. 3. Schematic stratigraphic sections illustrating the age and relationships of volcanic and intrusive units within the Zedong terrane and samples analyzed herein. The locations of i–iv are shown in Fig. 2.

Zedong), a sequence of flows and tuffs with limestone blocks occurs above gabbro. The most continuous sequence lies on a mountain range located immediately west of Zedong township (Fig. 3(ii)). Here exposures of the Zedong terrane continue for 10 km along strike parallel to the Yarlung Tsangpo River. This overturned section begins with approximately 100 m of pillow lavas overlain by recrystallised red ribbon-bedded cherts. These are in turn conformably overlain by ~ 700 m of hornblende-phyric basaltic–andesite breccias, flows, dykes and rare tuff beds.

Granodiorite intrudes green cherty tuff at one locality near Zedong city (ZT-92) but at all other localities, contacts between plutons and volcanic units are either faulted or not exposed. Field relations nevertheless suggest that the plutonic rocks were co-magmatic with basaltic–andesite magmatism. Dacite dykes also intrude the basaltic–andesite breccia and tuff units (Fig. 3).

3.4. Sampling strategy and preparation

Approximately half of the samples examined are volcanic in origin. The rest are from calc-alkaline plutons that either intrude the volcanic section (ZT-92) or are in fault contact with it. Basaltic–andesite dykes appear to be co-magmatic with a hornblende gabbro (sample ZT-224) that they cut.

Most of the zircon-poor volcanic strata from the Zedong terrane are metamorphosed to sub-greenschist facies (prehnite–calcite–epidote–albite–quartz) and hence unsuited for geochronologic study. Although we were able to identify one relatively unaltered hornblende-phyric autoclastic andesitic breccia, most of our effort has focused upon coarser grained, co-magmatic rhyolitic and andesitic dikes that are less affected by the metamorphism and are ubiquitous throughout the upper portion of the section (Aitchison et al., 2000). The plutonic rocks examined range from hornblende gabbro to quartz diorite and are representative of the intrusions found within this portion of the Zedong terrane. The relative stratigraphic positions of samples are shown on the schematic sections in Fig. 3.

Zircon and hornblende were extracted from samples using conventional crushing, sizing, magnetic and density methods. Six samples were selected for U–Pb analysis (see Fig. 4). Samples ZT-629 (dacite

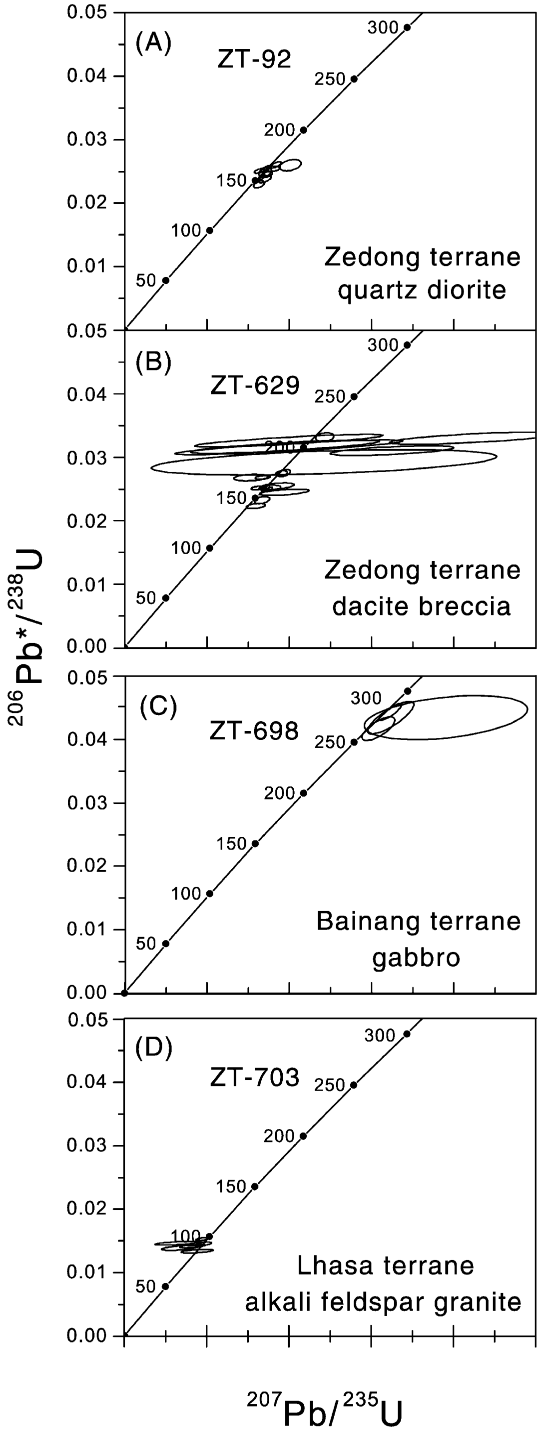

Fig. 4. Representative U–Pb concordia plot for ion–microprobe zircon analyses from the Zedong terrane and adjacent terranes.

breccia) and ZT-261 (dacite dyke) are volcanic while ZT-92, ZT-637, ZT-703 and ZT-698 are all plutonic. Zircons extracted from these samples are typically 50–150 μm in length and vary in habit from prismatic euhedral grains (ZT-629, ZT-703, ZT-698) to irregular fragments. Only three of the samples produced abundant zircons. Zircon is sparse in the remaining samples and several additional rocks that we attempted to extract zircons from yielded no usable grains.

Seven samples were selected for $^{40}Ar/^{39}Ar$ analysis of hornblende. Most of these are andesitic dikes from which no zircon was observed. The hornblende grains (180–250 μm) were ultrasonically cleaned and hand-selected to assure purity. Based upon binocular microscope inspection, they appeared > 99% pure of contaminant phases with adhering quartz and plagioclase feldspar representing the chief impurity. No K-rich mica was observed.

3.5. Ion microprobe analysis

U–Pb zircon analysis of zircon was performed using the UCLA CAMECA ims 1270 ion microprobe (Harrison et al., 2000; Quidelleur et al., 1997). Zircon grains were mounted in epoxy, polished to 1 μm, and coated with ~ 100 Å of Au. These analyses utilized a 5 nA primary O^- beam focused to a ~ 15 × 25 μm spot. The ion microprobe was operated at a mass resolving power of 6000 with an energy window of 50 eV. A 10-eV offset was used for $^{238}U^+$ relative to UO^+ and the Pb^+ peaks to compensate for contrasting energy distributions. Oxygen flooding of the sample surface at 3×10^{-5} Torr was employed to increase Pb^+ yields. U–Pb relative sensitivity factors were determined from a working curve (UO/U vs. Pb/U) defined by the measurement of standard zircon AS-3 which yields concordant $^{206}Pb/^{238}U$ and $^{207}Pb/^{235}U$ ages of 1099.1 ± 0.5 Ma by conventional methods (Paces and Miller, 1993).

3.6. $^{40}Ar/^{39}Ar$ step-heating

Hornblende concentrates (~ 20 mg) were wrapped in copper foil and packed along with Fish Canyon sanidine flux monitors in quartz tubes that were evacuated and sealed. Samples were irradiated for 45 hours in the L67 position of the Ford reactor (University of Michigan). Values of *J* calculated assuming an age of 27.8 ± 0.3 Ma for Fish Canyon sanidine varied between 0.00721 and 0.00719 depending upon sample position. Correction factors determined from K_2SO_4 and CaF_2 were $^{40}Ar/^{39}Ar_K = 0.0234$, $^{38}Ar/^{39}Ar_K = 0.0118$, $^{36}Ar/^{37}Ar_{Ca} = 0.00029$ and $^{39}Ar/^{37}Ar_{Ca} = 0.00085$. Typical m/e 36, 37, 38, 39 and 40 backgrounds were 1.1×10^{-17}, 1.6×10^{-17}, 1.2×10^{-17}, 3.1×10^{-17} and 24×10^{-17} mol, respectively. Measured atmospheric $^{40}Ar/^{36}Ar$ was 297.4 ± 0.8. Step-heating was conducted with a double vacuum Ta furnace. Argon isotopic measurements were performed using an automated VG1200S mass spectrometer (Quidelleur et al., 1997). Apparent ages are calculated using conventional decay constants and isotopic abundances (Steiger and Jager, 1977).

4. Results

Analytical results are summarized in Table 1. Complete data tables and supplementary plots are available from http://oro.ess.ucla.edu/labdata/data_repository.html.

4.1. U–Pb ion microprobe analysis of zircon

Zircon results are summarized in Fig. 4. For samples for which sufficient data could be gathered, we have calculated U–Pb ages in two ways. Weighted mean $^{206}Pb/^{238}U$ ages were determined from individual analyses that were corrected using ^{204}Pb as a proxy for common lead (see Table 1). The calculated uncertainties have been scaled by the square root of the MSWD to ensure that they reflect a realistic age dispersion. We have also calculated concordia intercept ages by least squares regression of individual analyses uncorrected for common lead (see Harrison et al., 2000). Provided that the U–Pb systematics within the zircons are concordant, the intercept of this array with concordia yields the crystallization age while the slope is proportional to common $^{207}Pb/^{206}Pb$ contaminating the analysis. For samples in which less than three analyses could be obtained, we report only the mean age.

In the case of ZT-92, the dispersion of ages is similar to our ability to reproduce U–Pb data for the standard AS-3 zircon on this day (± 1%). The significantly greater dispersion associated with ZT-629

Table 1
Summary of geochronologic results from the Zedong

Sample	Lithology	U–Pb age			$^{40}Ar/^{39}Ar$ age	
		N_i/N_a[a]	Weighted mean $^{206}Pb/^{238}U \pm 1\sigma$ (Ma)[b]	Concordia intercept $\pm 1\sigma$ (Ma)[c]	Total gas (Ma)[d]	Weighted mean (high Ca/K) $\pm 1\sigma$ (Ma)[e]
Zedong terrane						
ZT-19	basalt autobreccia	–	–	–	150.8	154.2 ± 2.1
ZT-261	dacite dyke	2/2	162.5 ± 5.9	–	–	–
ZT-229	basaltic-andesite dyke	–	–	–	153.0	155.8 ± 1.7
ZT-367	basalt dyke	–	–	–	155.1	156.1 ± 0.4
ZT-629	dacite breccia clast	13/22	161.9 ± 2.3	162 ± 2.6	–	–
ZT-629a	basalt dyke		–	–	144.6	152.2 ± 3.3
ZT-715	basaltic-andesite dyke		–	–	143.9	155.0 ± 1.1
ZT-92	quartz diorite	10/11	157.2 ± 1.8	157.9 ± 1.9	154.0	158.8 ± 1.2
ZT-224	hornblende gabbro	–	–	–	154.7	155.8 ± 2.0
ZT-637	quartz diorite	1/1	163.3 ± 5.0	–	–	–
Faulted blocks from other terranes incorporated in melange						
ZT-698	gabbro (Bainang)	4/4	273 ± 6	269 ± 6	–	–
ZT-703	alkali-feldspar granite (Lhasa)	7/7	92.4 ± 1.4	92.6 ± 1.8	–	–

[a] N_i = grains included, N_a = grains analyzed.
[b] Corrected using ^{204}Pb to estimate common lead ($^{206}Pb/^{204}Pb_{common}$ = 18.7).
[c] Intercept age determined by least squares regression through data uncorrected for common lead.
[d] Determined by weighting ages of individual steps by amount of ^{39}Ar released.
[e] Considers only high-temperature gas characterized by high Ca/K.

reflects both a more poorly defined calibration (± 3%) but also potentially unresolved contamination from inherited component. More than one third of the analyses from ZT-629 yield a $^{206}Pb/^{238}U$ age of 199 ± 3 Ma (1σ). Although only a few results were obtained from the two remaining samples, the calculated ages are consistent with hornblende $^{40}Ar/^{39}Ar$ ages from adjacent rocks. Finally, results from faulted plutonic rocks from adjacent terranes are well defined and well resolved, in terms of their U–Pb age, from rocks of the Zedong terrane.

U–Pb ages were also obtained for zircons from two samples of unknown tectonic affinity (ZT-698 and ZT-703). The first sample, ZT-703, is from an alkali feldspar granite that is tectonically juxtaposed between the Zedong terrane and the Luobusa Formation. It has a U–Pb age of 92.4 ± 1.4, which is within the range of previously reported ages for Gangdese type granitoids (Harrison et al., 2000). The second sample, ZT-698, is from a gabbro block that is tectonically overlain by sheared pillow lavas within the fault zone between the Bainang and Indian terranes. The U–Pb age of zircons contained within it (273 ± 6 Ma) is significantly older than any Tethyan oceanic material previously reported from the YTSZ.

4.2. $^{40}Ar/^{39}Ar$ step-heating of hornblende

Hornblende step-heating results from Zedong terrane samples are summarized in Fig. 5 with total fusion ages listed in Table 1. At low temperature, all samples yield gas characterized by low Ca/K, which we interpret as originating from an intergrown K-rich phase formed during lower grade metamorphism (Baldwin and Harrison, 1992; Ross and Sharp, 1988). The segment of ^{39}Ar release affected varies from less than 5% to over 40%. As expected for calcic amphiboles affected by subsequent recrystallization producing K-rich mica, the form of the Ca/K spectra correlate strongly with the age spectra. Specifically, apparent ages yielded by low-temperature gas release tend to be significantly younger than those yielded by subsequent higher temperature degassing). Accordingly, we have ignored the low-temperature steps in interpreting igneous ages from our $^{40}Ar/^{39}Ar$ results. Weighted mean ages presented in Table 1 are calcu-

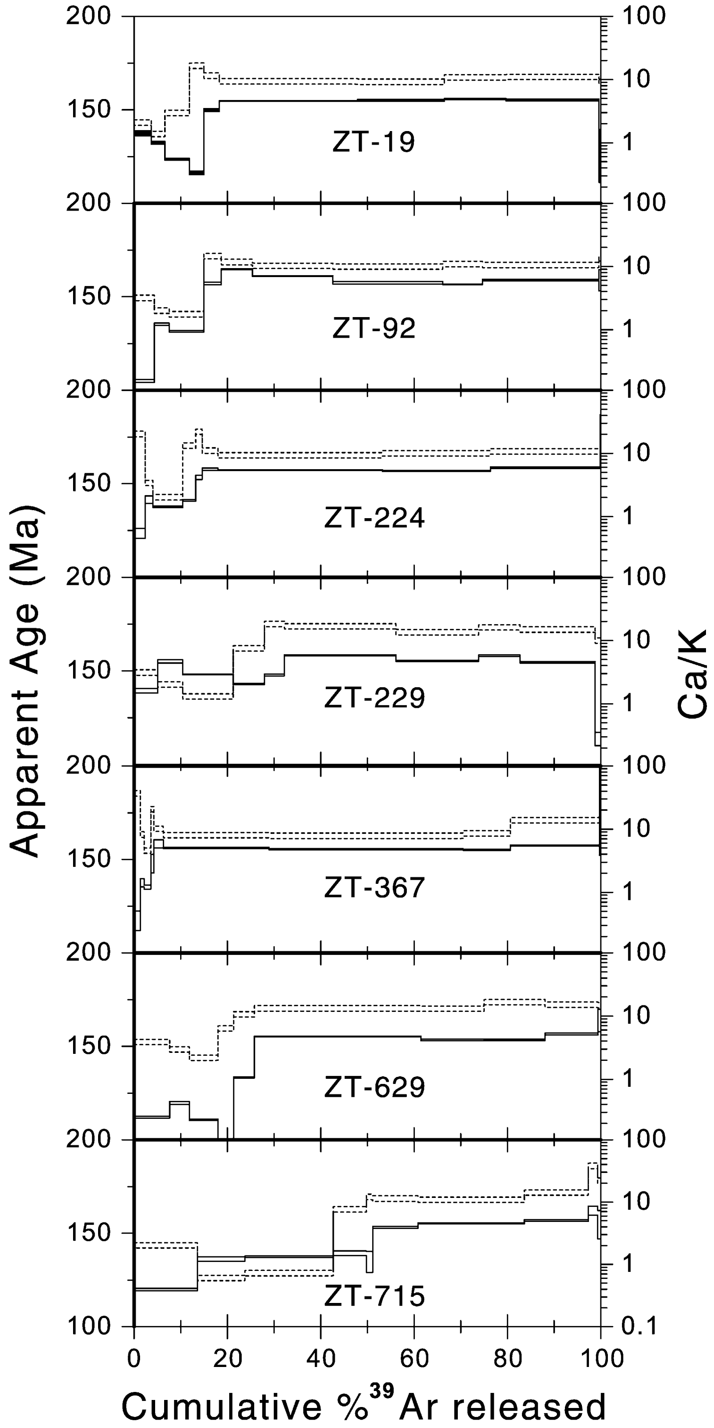

Fig. 5. $^{40}Ar/^{39}Ar$ age spectra for cumulative ^{39}Ar release (solid lines) and Ca/K ratio for ^{39}Ar release (dashed lines), from Zedong terrane samples.

lated only from steps with high Ca/K typical of igneous hornblende [Ca/K> ~ 10; (McDougall and Harrison, 1999)]. Note that we have scaled standard errors in Table 1 by the square root of the MSWD to more accurately represent the variability of the results. The resulting ages range from 152 to 159 Ma and yield an overall weighted mean age of 156.1 ± 0.3 ($\pm 1\sigma$) with an MSWD of 1.4.

5. Discussion

The Zedong terrane was previously reported to be Lower Cretaceous on the basis of fossil evidence reported by local workers (Badengzhu, 1979). Similarly, Lower Cretaceous fossils have been obtained from the Dazhuqu and Bainang terranes. For example, an upper Barremian to upper Aptian–lower Albian succession of supra-ophiolite sediments dated by radiolarian fossils overlies pillow lavas and pillow breccias of the Dazhuqu terrane at Xigaze (Zyabrev et al., 1999). While radiolarians and conodonts from red ribbon-bedded cherts from the Bainang terrane are Triassic to Jurassic and even Lower Cretaceous (Ziabrev et al., 2001; Bally et al., 1980; Wu, 1993), fine-grained clastic sediments overlying the cherts at Bainang are typically mid Cretaceous (mid Aptian) (Zyabrev et al., 2000). This evidence led Aitchison et al. (2000) to conclude that the arc and related intra-oceanic subduction system was active from at least the Early to mid Cretaceous.

Our new results indicate that subduction-related volcanism was active much earlier. The reported Lower Cretaceous fossils from the Zedong terrane were collected from volcaniclastic units that overlie the andesitic volcanics we have studied (Badengzhu, 1979). The $^{40}Ar/^{39}Ar$ and U–Pb results presented here indicate ages between 152 and 156 Ma for the dominant basaltic-andesite lithologies of the Zedong terrane. These results clearly indicate that arc construction was ongoing during the Late Jurassic. In fact, because the samples were taken from near the top of the sequence, the results seem to require that the Zedong terrane is Late Jurassic or older. Hornblende and quartz diorites that yield 155–159 Ma ages intrude or are faulted against andesite, indicating that pluton emplacement and basaltic-andesite magmatism were concurrent.

Once the oceanic lithosphere between India and the intra-Tethyan subduction zone was consumed, remnants of the island arc were emplaced onto the Indian margin. Additional oceanic lithosphere lay north of the accreting arc and subduction of this material continued beneath the Asian margin. During the Late Cretaceous through Mid-Oligocene this continued north-directed subduction resulted in the formation of the Gangdese batholith and eruptive rocks of the Lhasa terrane. In the late Paleogene the Indian Plate, now carrying the extinct intra-oceanic arc, collided with the Asian margin, initiating the Himalayan–Tibet orogeny, and ultimately creating the Yarlung–Tsangpo suture zone.

Finally, this new evidence for long-lived oceanic subduction (Middle Jurassic–Middle Cretaceous) may have important implications for the heterogeneity of the mantle underlying the Indo-Asian collision zone. For example, a considerable length of now-abandoned lithospheric material that is interpreted to exist beneath the Indo-Asian collision zone on the basis of tomographic imaging studies (Van der Voo et al., 1999) may have been produced by intra-oceanic subduction in Tethys.

Acknowledgements

The work described in this paper was supported by grants to J. Aitchison from the Research Grants Council of the Hong Kong Special Administrative Region, China (Project nos. HKU7102/98P and HKU 7299/99P). T.M. Harrison and M. Grove wish to acknowledge funding from NSF and the DoE. We also wish to thank Jessica D'Andrea, Eric Cowgill and Chris Coath who assisted in sample preparation and ion microprobe analysis. We appreciate the constructive reviews from Bradley Hacker and Philippe Matte, who helped improve the manuscript.

References

Abrajevitch, A., Aitchison, J.C., Ali, J.R., 2001. Paleomagnetism of the Dazhuqu Terrane, Yarlung–Zangbo Suture Zone, Southern Tibet. EOS, Transactions, American Geophysical Union Fall Meeting Supplement. Abstract GP11A-0188.

Aitchison, J.C., Badengzhu, Davis, A.M., Liu, J., Luo, H., Malpas, J., McDermid, I., Wu, H., Ziabrev, S., Zhou, M.F., 2000. Remnants of a Cretaceous intra-oceanic subduction system within the Yarlung–Zangbo suture (southern Tibet). Earth Planet. Sci. Lett. 183, 231–244.

Aitchison, J.C., Davis, A.M., Badengzhu, Luo, H., 2002. The Lower Miocene Gangrinboche conglomerates, Yarlung–Tsangpo suture zone, SE Tibet. J. Asian Earth Sci., in press.

Badengzhu, 1979. (Compiler) Xizang Autonomous Region Zhanang–Sangri Regional Geology Reconnaissance Map 1:50,000. Xizang Geological Survey Geological Team #2, Group 2. Lhasa.

Baldwin, S.L., Harrison, T.M., 1992. The P–T–t history of blocks in serpentinite-matrix melange, west-central Baja California. Geol. Soc. Am. Bull. 104, 18–31.

Bally, A.W., Allen, C.R., Geyer, R.B., Hamilton, W.B., Hopson, C.A., Molnar, P.H., Oliver, J.E., Opdyke, N.D., Plafker, G., Wu, F.T., 1980. Notes on the geology of Tibet and adjacent areas; report of the American plate tectonics delegation to the People's Republic of China. Open-File Rep.-U. S. Geol. Surv. U.S. Geological Survey, Reston, VA, United States 101 pp.

Corfield, R.I., Searle, M.P., Pederson, R.B., 2001. Tectonic Setting, Origin, and Obduction History of the Spontang Ophiolite, Ladakh Himalaya, NW India. J. Geol. 109, 715–736.

Gansser, A., 1964. The Geology of the Himalaya. Wiley, New York, 289 pp.

Girardeau, J., Mercier, J.C., Xibin, W., 1985. Petrology of the mafic rocks of the Xigaze ophiolite, Tibet; implications for the genesis of the oceanic lithosphere. Contrib. Mineral. Petrol. 90 (4), 309–321.

Harrison, T.M., Yin, A., Grove, M., Lovera, O.M., Ryerson, F.J., Zhou, X., 2000. The Zedong Window: a record of superposed Tertiary convergence in southeastern Tibet. J. Geophys. Res. 105 (B8), 19211–19230.

Heim, A., Gansser, A., 1939. Central Himalaya; Geological Observations of the Swiss Expedition 1936. Gebruder Fretz, Zurich, 246 pp.

Hérbert, R., Beaudoin, G., Varfalvy, V., Huot, F., Wang, C.S., Liu, Z.F., 2000. Yarlung Zangbo ophiolites, southern Tibet revisited. 15th Himalaya-Karakorum-Tibet workshop abstracts. Earth Sci. Front. 7 (118), 124–126.

McDermid, I.R.C., Aitchison, J.C., Badengzhu, Davis, A.M., 2001. The Zedong terrane: an intra-oceanic magmatic arc assemblage, Tibet. 16th Himalaya-Karakoram-Tibet workshop abstracts. J. Asian Earth Sci. 19 (3A), 44.

McDermid, I.R.C., Aitchison, J.C., Badengzhu, Davis, A.M., Lou, H., Ziabrev, S., 2002. A Jurassic intra-oceanic are rift, south Tibet, in preparation.

McDougall, I., Harrison, T.M., 1999. Geochronology and Thermochronology by the $^{40}Ar/^{39}Ar$ Method. Oxford Univ. Press, New York, 261 pp.

Paces, J.B., Miller, J.D., 1993. Precise U–Pb age of Duluth Complex and related mafic intrusions, northeastern Minnesota: Geochronological insights into physical, petrogenetic, paleomagnetic, and tectonomagmatic processes associated with the 1.1 Ga midcontinent rift system. J. Geophys. Res. 98, 13997–14013.

Pearce, J.A., Deng, W., 1988. The ophiolites of the Tibet Geotraverses, Lhasa to Golmud (1985) and Lhasa to Kathmandu (1986). Philos. Trans. R. Soc. London, Ser. A 327 (1594), 215–238.

Pedersen, R.B., Searle, M.P., Corfield, R.I., 2001. U–Pb zircon ages from the Spontang Ophiolite, Ladakh Himalaya. J. Geol. Soc. (London) 158, 513–520.

Quidelleur, X., Grove, M., Lovera, O.M., Harrison, T.M., Yia, A., Ryerson, R.J., 1997. Thermal evolution and slip history of the Renbu Zedong Thrust, southeastern Tibet. J. Geophys. Res., B 102 (2), 2659–2679.

Ross, J.A., Sharp, W.D., 1988. The effects of sub-blocking temperature metamorphism on the K/Ar systematics of hornblende: $^{40}Ar/^{39}Ar$ dating of hornblende of polymetamorphic garnet amphibolite from the Franciscan Complex, California. Contrib. Mineral. Petrol. 10, 213–221.

Searle, M.P., Asif, M., Khan, M., Fraser, J.E., Gough, S.J., Qasim Jan, M., 1999. The tectonic evolution of the Kohistan–Karakoram collision belt along the Karakoram Highway transect, north Pakistan. Tectonics 18 (6), 929–949.

Steiger, R.H., Jager, E., 1977. Convention on the use of decay constants in geo- and cosmochronology. Earth Planet. Sci. Lett. 36, 359–362.

Van der Voo, R., Spakman, W., Bijwaard, H., 1999. Tethyan subducted slabs under India. Earth Planet. Sci. Lett. 171, 7–20.

Wu, H.R., 1993. Upper Jurassic and Lower Cretaceous radiolarians of Xialu chert, Yarlung Zangbo ophiolite belt, southern Tibet. In: Blueford, J.R., Murchey, B.L. (Eds.), Radiolaria of Giant and Subgiant Fields of Asia, Nazarov Memorial Volume. Micropaleontology, Spec. Pap., vol. 6. Micropaleontology Press, American Museum of Natural History, New York, USA, pp. 115–136.

Yin, A., Harrison, T.M., Ryerson, F.J., Chen, W.J., Kidd, W.S.F., Copeland, P., 1994. Tertiary structural evolution of the Gangdese thrust system in southeastern Tibet. J. Geophy. Res. 99, 18175–18201.

Yin, A., Harrison, T.M., Murphy, M.A., Grove, M., Nie, S., Ryerson, F.J., Wang, X.F., Chen, Z.L., 1999. Tertiary deformation history of southeastern and southwestern Tibet during the Indo-Asian collision. Geol. Soc. Am. Bull. 111, 1644–1664.

Zhou, M.F., Robinson, P.T., Malpas, J., Li, Z., 1996. Podiform chromitites in the Luobusa Ophiolite (southern Tibet); implications for melt-rock interaction and chromite segregation in the upper mantle. J. Petrol. 37 (1), 3–21.

Ziabrev, S.V., Aitchison, J.C., Badengzhu, Davis, A.M., Luo, H., Liu, J.B., 2001. More about the missing Tethys in the Yarlung–Tsangpo. 16th Himalaya-Karakoram-Tibet workshop abstracts. J. Asian Earth Sci. 19 (3A), 82–83.

Zyabrev, S.V., Aitchison, J.C., Badengzhu, Davis, A.M., Luo, H., Malpas, J., 1999. Radiolarian biostratigraphy of supra-ophiolite sequences in the Xigaze area, Yarlung–Tsangpo suture, Southern Tibet (preliminary report). Radiolaria 17, 13–19.

Zyabrev, S.V., Aitchison, J.C., Badengzhu, Davis, A.M., Luo, H., Liu, J.B., 2000. Tethyan relics in the Yarlung–Tsangpo suture, Tibet: structural setting, radiolarian ages and their tectonic significance. Ninth Meeting of the International Association of Radiolarian Paleontologists, INTERRAD 2000, Program with Abstracts 72.